VI International Conference on Adaptive Modeling and Simulation
ADMOS 2013
J. P. Moitinho de Almeida, P. Díez, C. Tiago and N. Parés (Eds)

A FULLY COUPLED FINITE VOLUME SOLVER FOR THE SOLUTION OF INCOMPRESSIBLE FLOWS ON LOCALLY REFINED NON-MATCHING BLOCK-STRUCTURED GRIDS

Ulrich Falk, Michael Schäfer

Institute of Numerical Methods in Mechanical Engineering
Technical University Darmstadt
Dolivostraße 15, 64293 Darmstadt, Germany
e-mail: falk/schaefer@fnb.tu-darmstadt.de, www.fnb.tu-darmstadt.de

Key words: computational fluid dynamics, finite volume method, pressure-based coupled solver, block-structured grid, non-matching block interface

Abstract. A fully coupled solver for the solution of steady laminar incompressible flow problems on locally refined non-matching block-structured grids that promises improved convergence properties is presented. For this a coupled velocity-pressure algorithm developed by Darwish [1] that solves the momentum and pressure equations simultaneously is extended correspondingly. The spatial finite-volume discretisation applied is of second-order accuracy. All blocks are implicitly coupled and the method is fully conservative.
The newly developed method is verified via comparisons with manufactured solutions. Its performance is evaluated by systematic comparisons with standard segregated pressure-correction solution techniques for representative test cases.

1 INTRODUCTION

Incompressible flows of Newtonian fluids can be described mathematically by the non-linear Navier-Stokes equations. To handle these equations in the present approach numerically, they are discretised with a finite volume method on collocated block-structured grids.
Geometrically complicated flow configurations demand highly adapted grids in order to achieve the required numerical accuracy. In general the grid should be very fine in regions with larger variations of the dependent variables. Choosing the grid resolution of a block-structured grid such as large variations of the dependent variables are sufficiently resolved, can lead to high densities of grid points in regions where they are not required. One possibility to avoid regions with too high grid resolution are local grid refinement approaches. Various strategies for local grid refinement have been proposed in literature [3].

The present approach constitutes a h-method where the grid cells are obtained by dividing the control volumes (CVs) into four subcells in two dimensions and eight subcells in three dimensions. The approach can be easily extended to an arbitrary refinement of grid cells. A block-wise refinement of the block-structured grid is performed.
There are mainly two strategies to couple the local refinement region with the non-refined regions: The first one treats the refinement region as a different grid level and the result on a coarse level serves as a boundary condition and an initial guess to the computation of a finer level. In case of a rather complex multigrid datastructure is already used such approaches are fairly easy to implement due to the preservation of the grid structure and straightforward treatment of the coarse-fine interface. Based on the idea of Berger and Collela [4] Quirk [5] successfully implemented an hierarchical adaptive grid refinement approach for compressible flows.
The second strategy couples refined and non-refined regions at the same level, computing the whole grid simultaneously [6, 7]. Special discretisation schemes are required for the coarse-fine grid interface to ensure a proper coupling of the subdomains. The presented algorithm follows this second strategy.
There are several ways by which blocks can be interconnected. Arbitrary overlapping blocks connected to each other can be generated during a grid generation process (so-called Chimera grids). With these Chimera grids it is difficult to ensure conservation. Interpolation between overlapping regions may have to be constructed problem dependent, restricting the generality of the algorithm.
In the presented approach the internal block boundaries are patched together, making them share a common interface line, but allowing a different point distribution for each block. Compared to Chimera grids redundant regions are avoided. These patched grids are also called zonal grids or block adaptive grids.
Besides the choice of the grid the velocity-pressure coupling algorithm is an essential part with respect to the efficiency and robustness of a solution algorithm for the Navier-Stokes equations. There are mainly two strategies to perform the velocity-pressure coupling on collocated grids, either a segregated or a coupled approach. In the segregated approach, the system of equations for all variables are solved sequentially using fixed values from the last iteration of other dependent variables. A well known representative is the SIMPLE algorithm [8].
In the coupled approach all discretised equations of all dependent variables are solved in one system. Pressure based coupled solvers can be divided into two groups. In the first group the Navier-Stokes equations are discretised in a straightforward manner, i.e., no pressure variable in the mass-conservation equation is introduced. An example for this group is Vankas [10] symmetric coupled Gauss Seidel algorithm. These approaches lead to an ill-conditioned system of equations because of the present zeros in the main diagonal of the continuity equation. The solution of these stiff algebraic equation systems is rather difficult.
In the second group, which includes the approach presented here, a pressure equation is

derived in the same way as in the SIMPLE algorithm. Examples of this group are Lonsdale's [11] control-volume finite element method and the method of Webster [12]. In the presented approach the velocity-pressure coupling on collocated structured grids developed by Darwish [1] is extended to non-matching block-structured grids. The extention allows the specific adaptation of the numerical grid for each flow configuration.
The local block refinement (LBR) method described in this paper is aimed at increasing accuracy and efficiency in the computation of flow problems. The general discretisation procedure for the coupled approach is first outlined in the next section, followed by a description of the refinement method in section 3. In section 4 the LBR method is verified via Manufactured Solutions. In section 5 the performance is evaluated by systematic comparison with standard segregated pressure-correction solution techniques for representative test cases.

2 DISCRETISATION PROCEDURE

Laminar incompressible steady flows of Newtonian fluids can be described by the following nonlinear partial differential equations describing conservation of mass and momentum:

$$\frac{\partial u_i}{\partial x_i} = 0 \tag{1}$$

$$\frac{\partial(\rho u_i\, u_j)}{\partial x_j} = \frac{\partial}{\partial x_j}\left[\mu\left(\frac{\partial u_i}{\partial x_j} + \frac{\partial u_j}{\partial x_i}\right)\right] - \frac{\partial p}{\partial x_i} + \rho f_i \tag{2}$$

where u_i denotes the components of the velocity vector, x_i is the vector of Cartesian coordinates, μ the dynamic viscosity, p the pressure and f_i the outer force vector.
The governing equations (1) and (2) are solved via the block-structured finite volume method, whereby the flow domain is divided into blocks and each block is discretised by a structured grid. Each control volume is associated with a main grid point at its geometric center. To calculate the balance of the conserved quantities, the governing equations are integrated over each CV. Through the use of the divergence theorem the volume integrals of the convection, diffusion and pressure gradient terms are transferred to surface integrals, which, with the application of the continuity equation and application of approximation schemes of second order accuracy for the surface and volume integrals (mid-point rule), results in:

$$\sum_{f=nb(P)} \rho_f u_{i,f} n_{i,f} S_f = 0 \tag{3}$$

$$\sum_{f=nb(P)} \left[\rho_f\, u_{i,f}\, u_{j,f}\, n_{j,f} - \mu\left(\frac{\partial u_i}{\partial x_j}\right)_f n_{j,f} + p_f\, n_{i,f}\right] S_f = \rho\, f_{i,P}\, V_P \tag{4}$$

where variables with subscript f are CV-face variables, variables with subscript P are CV-center variables, S_f denotes the face area, n_f the unit cell-face normal vector and V_P

the cell volume.
To yield an algebraic equation system for the momentum equations the variation of the dependent variables and its derivatives have to be expressed in terms of grid-point center values. The diffusive fluxes are discretised by a central differential scheme (CDS), the convective fluxes are treated with a so called deferred correction approach, i.e. a first-order-upwind approximation (UDS) is used to calculate the elements of the coefficient matrix while the explicitly calculated difference between the UDS and CDS approximation is added on the right hand side of the equation system. The overall approximation order (formal order of accuracy) is therefore second order.
Starting point for the derivation of the pressure equation is the equation of mass conservation. The mass flow through a CV-face emerges from the product of face-velocity, density and the face-area. The aim is to express the face-velocity by means of pressure and center-point-velocities. This can be achieved by the construction of a pseudo-momentum equation at the CV-face. Therefore two momentum equations at, e.g. CV-mid-point P and the adjacent CV-mid-point F, are Rhie-Chow interpolated [13]. The face-velocity is obtained as

$$u_{f,i} = \underbrace{\overline{u_{f,i}}}_{\text{linear interpolated velocity}} \underbrace{- \overline{D_f} \left[\left(\frac{\partial p}{\partial x_i} \right)_f - \left(\overline{\frac{\partial p}{\partial x_i}} \right)_f \right]}_{\text{correction term}} \tag{5}$$

where $\overline{D_f}$ is the quotient of the cell volume and the corresponding coefficient of the main diagnonal of the discretised momentum equation (a_p^u, a_p^v, a_p^w). The variables with overbar in equation (5) are linearly interpolated cell face values from the neighboring cell centers. A detailed explanation of the derivation of the pressure equation can be found in [1]. The continuity equation then becomes

$$\sum_{f=nb(P)} \rho_f \left[\overline{u_{f,i}} - \overline{D_f} \left(\frac{\partial p}{\partial x_i} \right)_f \right] n_{i,f} S_f = - \sum_{f=nb(P)} \rho_f \overline{D_f} \left(\overline{\frac{\partial p}{\partial x_i}} \right)_f n_{i,f} S_f. \tag{6}$$

The variables on the left hand side of equation (4) and (6) are treated implicitly. This is the cornerstone of the coupled algorithm and can accelerate the convergence.
The discretised momentum equations (4) are linearized using values for mass fluxes from the previous iteration. The PETSc linear algebra library [14] (preconditioned Generalized Minimal Residual Krylov method) is used to solve the resulting sparse linear system.

3 LOCAL BLOCK REFINEMENT

At the interior of each block each CV has four neighbors in two dimensions or six neighbors in three dimensions which share a common face. At non-matching block interfaces this is not necessarily the case (see Figure 3). The aim is now to solve the conservation equations on a global grid, while the non-matching block interfaces should be treated

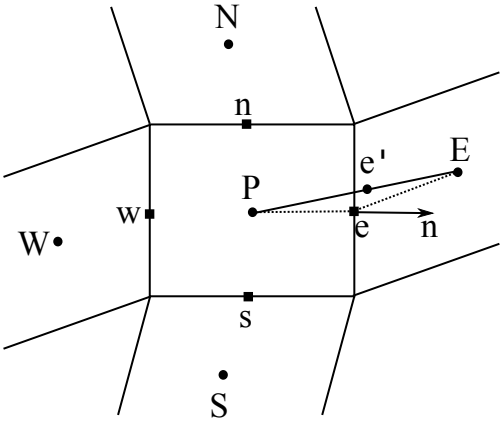

Figure 1: A typical CV and notation used.

implicitly, i.e. not by means of boundary conditions. The non-matching block interface treatment described below is based on Lilek's work [6] and was adjusted accordingly for the coupled approach of Darwish [1]. Since both surface and volume integrals are approx-

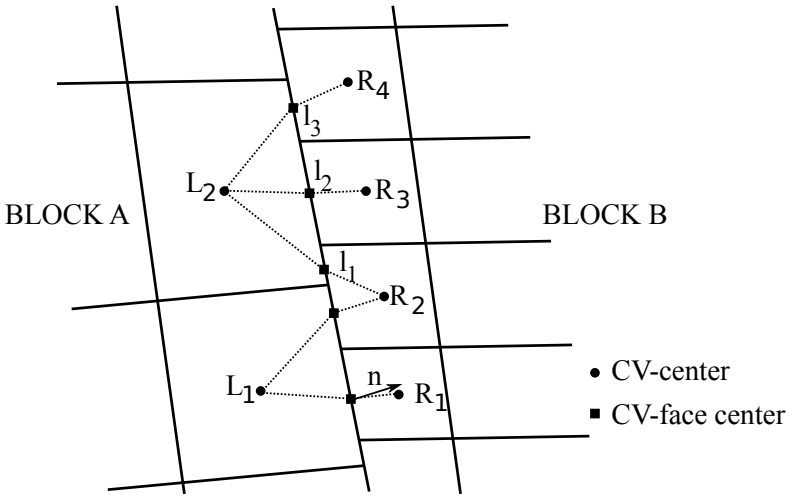

Figure 2: A typical non-matching block interface in two dimensions.

imated using the mid-point rule, nothing has to be changed for the calculation of volume integrals when non-matching block interfaces are present. However some adaptions have to be performed in order to approximate the surface integrals. When non-matching block interfaces are present a CV can have several adjacent neighboring CVs (see Figure 3, L2 has R2, R3 and R4 as neighbor) at the interface. According to the number of adjacent CVs, face value approximations (see Figure 3, l_1, l_2, l_3) for the convective, diffusive and pressure terms in the equations (4) and (6) have to be calculated. Details on various options to calculate these approximations can be found in Ferziger and Peric [15]. Here

only methods used in the present approximations will be described for the east side. The other CV-faces are treated accordingly. CV-face variables (u,v,w,p) are approximated using linear interpolation with a correction term to restore second-order accuracy on skewed grids (see Figure 1):

$$\sigma_e \approx \sigma_E \, \gamma_e \; + \; \sigma_P \; (1 - \gamma_e) \; + \; (\mathrm{grad}\, \sigma)_{e'} \cdot (r_e - r_{e'}) \tag{7}$$

with the linear interpolation factor γ_e, the linearly interpolated CV-face gradient in the CV-center $(\mathrm{grad}\, \sigma)_{e'}$ and the position vectors r_e and $r_{e'}$. The CV-center gradient can be calculated explicitly using the midpoint-rule approximation based on the Gauss theorem:

$$\left(\frac{\partial \sigma}{\partial x_i} \right)_P \approx \frac{\sum_k \sigma_k \, S_k^i}{V} \quad \text{with} \quad (k = e, w, n, s, \dots) \tag{8}$$

where σ_k is calculated in the same way as in equation (7). For the diffusive term the following second order accurate approximation is applied:

$$(\mathrm{grad}\, \sigma)_e \cdot n_e \approx \frac{\sigma_E - \sigma_P}{|r_E - r_P|} - \underline{\overline{(\mathrm{grad}\, \sigma)}_e^{old} \left(\frac{r_E - r_P}{|r_E - r_P|} - n_e \right)} \tag{9}$$

The underlined term is calculated using prevailing values of the variables. The explicitly calculated gradient at the CV face (denoted by the overbar) is obtained by linear interpolation of the CV-center gradients.
Correspondingly to the finite volume discretisation these approximations are multiplied by the overlapping CV area of the adjacent CVs, so that the conservativity is fulfilled.

4 VERIFICATION

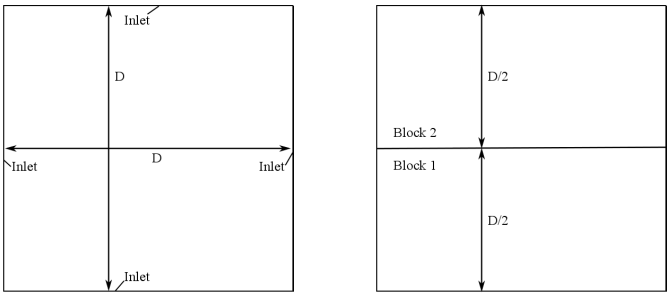

Figure 3: Manufactured Solution left: geometry and boundary conditions, right: applied blocking.

In this section it is demonstrated, that (i) the LBR method is correctly integrated in the coupled approach, (ii) the implemented LBR approach is stable for a higher refinement rate than two, (iii) it is possible to improve the solution accuracy with the implemented

LBR method and (iv) the obtained solution accuracy is identical to a segregated LBR approach presented in [6]. These mentioned points can be examined in a simple way using the Method of Manufactured Solutions (MMS) in a code verification process. The MMS is used to obtain exact solutions for the governing equations to determine whether the calculated solution is converging and the discretisation error is reduced at the expected rate (observed order equals formal order of accuracy). The form of the Manufactured Solution was chosen to be infinitely differentiable:

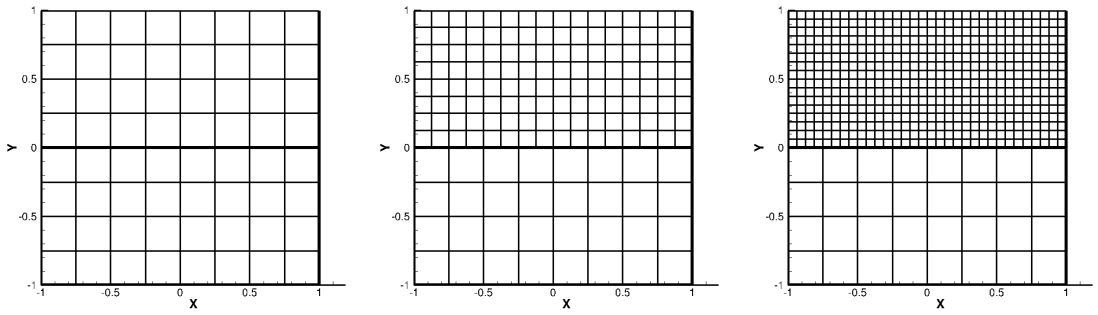

Figure 4: Examples of used grids in verification process; left: 2 blocks grid spacing 1/4, middle: 2 blocks grid spacing 1/4 & 1/8, right: 2 blocks grid spacing 1/4 & 1/16

$$
\begin{aligned}
u(x,y) &= -\cos(2\pi x)\sin(2\pi y) \\
v(x,y) &= \sin(2\pi x)\cos(2\pi y) \\
p(x,y) &= -\frac{1}{4}\left(\cos(4\pi x) + \cos(4\pi y)\right)
\end{aligned}
\tag{10}
$$

with x, y $\in [-1,1]^2$. Additional source terms after applying the Manufactured Solutions to the governing equations with density ρ and viscosity μ set to one are:

$$
\begin{aligned}
su(x,y) &= -8\pi^2\cos(2\pi x)\sin(2\pi y) \\
sv(x,y) &= 8\pi^2\sin(2\pi x)\cos(2\pi y)
\end{aligned}
\tag{11}
$$

where $su(x,y)$ is the source term for the u-momentum equation and $sv(x,y)$ is the source term for the v-momentum equation. The flow geometry, boundary conditions and the applied blocking are shown in Figure 3. Examples of applied grids are shown in Figure 4. Results obtained with different sequences of meshes are given in Tables 1 and 2. Due to the symmetry of the velocity components and therefore identical results concerning error and observed order of accuracy in the following the v-velocity component is omitted. The observed order of accurary is calculated by the following equation:

$$
\text{observed order} = \frac{\log\left(\varepsilon_{N/2}/\varepsilon_N\right)}{\log(2)} \tag{12}
$$

Table 1: Solution error and observed order (OO) of accuracy of u-velocity.

grid spacing	ε_N coupled	OO coupled	ε_N segregated	OO segregated
1/16	0.7643E-02	-	0.7646E-02	-
1/16 & 1/32	0.3840E-02	-	0.3842E-02	-
1/16 & 1/64	0.2001E-02	-	0.2015E-02	-
1/32	0.1906E-02	2.01	0.1906E-02	2.00
1/32 & 1/64	0.9621E-03	2.00	0.9596E-03	2.00
1/32 & 1/128	0.5043E-03	1.99	0.5069E-03	1.99
1/64	0.4761E-03	2.00	0.4761E-03	2.00
1/64 & 1/128	0.2395E-03	2.00	0.2399E-03	2.00
1/64 & 1/256	0.1265E-03	2.00	0.1272E-03	1.99

where N is the number of grid points and ε is the error defined by

$$\varepsilon_N = \sqrt{\frac{\sum_{i=1,NT} \left(\sigma_i - \sigma_{i,exact}\right)^2}{NT}}. \tag{13}$$

NT is the total number of grid cells and σ stands for the velocity-components and pressure. The results confirm, that (i) the approach is correctly implemented, (ii) the observed order

Table 2: Solution error and observed order (OO) of accuracy of pressure.

grid spacing	ε_N coupled	OO coupled	ε_N segregated	OO segregated
1/16	0.6261E-01	-	0.8658E-01	-
1/16 & 1/32	0.5287E-01	-	0.6019E-01	-
1/16 & 1/64	0.6575E-01	-	0.6789E-01	-
1/32	0.2015E-01	1.63	0.2062E-01	2.06
1/32 & 1/64	0.1421E-01	1.89	0.1541E-01	1.96
1/32 & 1/128	0.1398E-01	2.23	0.1470E-01	2.20
1/64	0.5287E-02	1.93	0.5317E-02	1.95
1/64 & 1/128	0.3687E-02	1.94	0.3808E-02	2.01
1/64 & 1/256	0.3344E-02	2.06	0.3844E-02	1.93

and formal order of accuracy agree independent of the refinement rate, (iii) it is possible to improve the numerical accuracy by local block-refinement and (iv) the solution error of the coupled and segregated approach is almost identical independent of the refinement rate.

5 APPLICATION

Separated flows behind a backward facing step have become an important test for CFD code developers. We use such a configuration to investigate possible performance gains through the application of LBR.
The geometry and applied blocking of the two-dimensional backward facing step flow is shown in Figure 5, where all length scales are given relative to the inflow height $D = 1\ m$. The kinematic viscosity $\nu = 10^{-3}\ m^2 s^{-1}$ and density of $\rho = 1.0\ kg\ m^{-3}$ is prescribed. At the inlet boundary a parabolic velocity profile is defined resulting in a steady flow at Re=200. Examples of applied grids are shown in Figure 6.

The physical quantity for comparison is the reattachment length X_{RL} of the flow behind

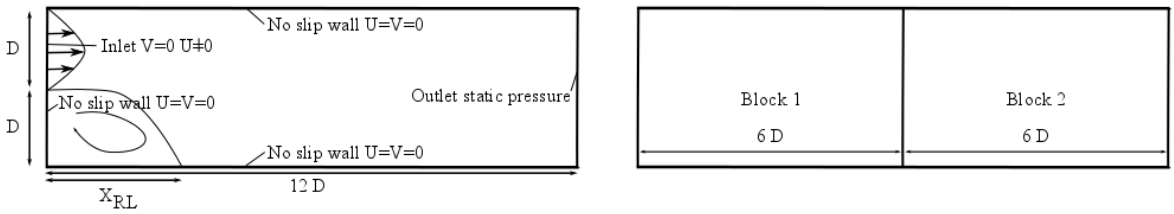

Figure 5: Backward facing step flow configuration left: geometry and boundary conditions, right: applied blocking.

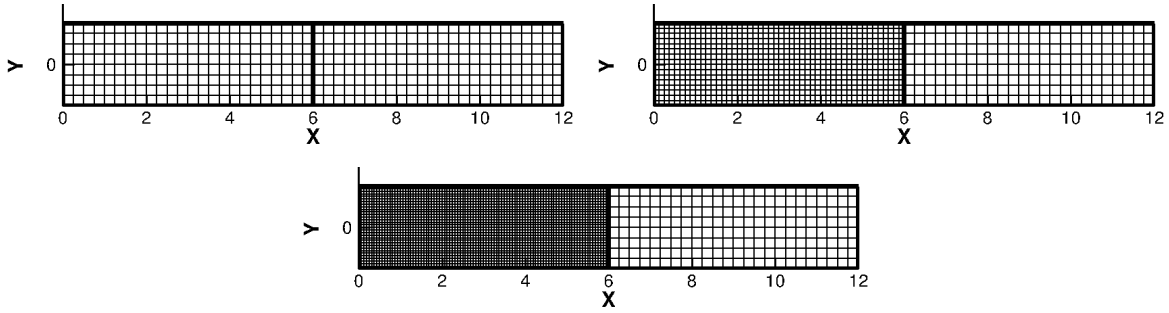

Figure 6: Examples of used grids backward facing step flow configuration left top: 2 blocks grid spacing 1/4, right top: 2 blocks grid spacing 1/8 & 1/4, bottom: 2 blocks grid spacing 1/16 & 1/4

the backward facing step. The results are summarized in Table 3 for various grids, where the coupled solver is called CP and the segregated solver is called SG. LBR indicates the application of local block refinement. Besides the reattachment length, the memory requirement, the total computing time and the computing time per CV are listed in Table 3 to allow a realistic comparison of the performance of both algorithms and the benefits through LBR. All computations were carried out on a workstation with Intel Core i7-960 CPU, 3.2 GHz and 5979 Mbyte memory. Since no exact solution for the stated flow problem is available, no quantitative statement about the error in the reattachment length can

Table 3: Results for backward facing step flow.

Code	Grid spacing	X_{RL} [m]	Memory [MB]	CPU time [sec]	CPU time/CV [sec]
CP	1/8	4.8597	16.71	1.20	0.0007839
	1/16	5.1599	48.06	4.50	0.0007325
	1/32	5.2585	189.76	22.78	0.0009273
	1/64	5.3003	822.35	130.67	0.0013293
CP LBR	1/16 & 1/8	5.1589	32.33	3.29	0.0008574
	1/32 & 1/16	5.2584	119.15	14.38	0.0009360
	1/64 & 1/32	5.2983	509.41	75.97	0.0012365
CP LBR	1/16 & 1/4	5.1515	29.44	4.42	0.0013543
	1/32 & 1/8	5.2572	105.82	15.27	0.0011701
	1/64 & 1/16	5.2989	448.52	74.30	0.0014228
SG	1/8	4.8613	3.14	2.15	0.0013985
	1/16	5.1612	4.21	23.54	0.0038309
	1/32	5.2601	8.56	308.12	0.0125375
	1/64	5.3008	25.41	4155.18	0.0422687
SG LBR	1/16 & 1/8	5.1593	3.70	12.49	0.0032512
	1/32 & 1/16	5.2595	6.82	151.28	0.0098488
	1/64 & 1/32	5.3008	18.92	2149.76	0.0349901
SG LBR	1/16 & 1/4	5.1521	3.56	9.51	0.0029156
	1/32 & 1/8	5.2572	5.77	123.47	0.0094570
	1/64 & 1/16	5.3002	14.81	1711.89	0.0327798

be given. However, the results show a good convergence behaviour. To access the benefit through LBR block one (see Figure 6) is always refined. Ideally, the reattachment length should be the same as if the fine grid spacing is applied for the entire domain.
The results in Table 3 demonstrate that the reattachment length X_{RL} is nearly independent of the grid refinement rate at the block interface. That means the reattachment length X_{RL} with the application of LBR is nearly the same as if the fine grid spacing is applied for the entire domain. This represents a saving of at most 46 per cent in the total number of CVs for a refinement rate of four. Therefore, the memory requirement, which can be a limiting factor for the application of the coupled approach, can be almost halved. Due to the smaller number of CVs and hence smaller computational effort needed per iteration, the computational time is reduced to 57 per cent of the computational time for a conventional grid. Therefore, the performance of the already highly efficient coupled approach could be increased significantly through the integration of the LBR approach. According to the results in Table 3 for the coupled approach a refinement rate greater two

offers no great benefit with respect to the computation time. It seems that an excessive non-orthogonality at the block interface for refinement rates greater two reduces the linear solver convergence to an extend that it cancels the advantage of the saving of CVs.
For completeness the results for the segregated solver are presented in Table 3 also. Generally speaking, the results are consistent with those of the coupled approach. The memory requirement and computing time can be reduced drastically through LBR in contrast to the coupled approach even for higher refinement rates.
The superiority of the coupled approach compared to the segregated approach could also be demonstrated for the integrated LBR approach. The results show that the CPU time per control volume are at least one magnitude shorter compared to the segregated approach.

6 CONCLUSIONS

The coupled approach introduced by Darwish [1] was successfully extended by a local grid refinement procedure. By means of Manufactured Solutions it was exemplified that the method proved to preserve second order accuracy of the underlying numerical scheme. Moreover, the local grid refinement was found to be robust even for higher refinement rates and provided substantial gains in performance and reduction of memory requirements. In the considered backward facing step case, computing time gains of 43 per cent and reduction of memory requirements up to 45 per cent could be verified.
Although the implementation and results presented correspond to the two-dimensional version of the code, the extension of the procedure to three dimensions is straight forward. For the three-dimensional local block refinement procedure even larger gains in performance and reduction of memory requirements are expected.

REFERENCES

[1] Darwish M.; Sraj, I. and Moukalled, F., A coupled incompressible flow solver on structured grids. *Numerical Heat Transfer, Part B* (2007) **52**:352-371.

[2] M. Schäfer, *Computational Engineering - Introduction to numerical methods*, Springer, Berlin, 2006.

[3] Lange C. F.; Schäfer M. and Durst F., Local refinement with a multigrid flow solver. *International Journal for Numerical Methods in Fluids* (2002) **38**:21-41.

[4] Berger M.J. and Collela P., Local adaptive mesh refinement for shock hydrodynamics. *Journal of Computational Physics* (1989) **82**:64-84.

[5] Quirk J.J., A cartesian grid approach with hierarchical refinement for compressible flows. *Proceedings of the Second European Computational Fluid Dynamic Conference, Stuttgart* (1994) Wiley: Chichester:200-209.

[6] Lilek Z.; Muzaferija S. and Peric M., An implicit finite-volume method using non-matching blocks of structured grid. *Numerical Heat Transfer, Part B: Fundamentals* (1997) **32,4**:385-401.

[7] Coelho P.; Pereira J.C.F. and Carvalho M.G., Calculation of laminar recirculating flows using local non-staggered grid refinement system. *International Journal for Numerical Methods in Fluids* (1991) **12**:535-557.

[8] Patankar S.V. and Spalding D.B., A calculation procedure for heat, mass and momentum transfer in three-dimensional parabolic flows. *International Journal Heat and Mass Transfer* (1972) **15**:1787-1806.

[9] Moukalled F. and Darwish M., A unified formulation of the segregated class of algorithms for fluid flow at all speeds. *Numerical Heat Transfer B* (2000) **37**:103-139.

[10] Vanka S.P., Fully coupled calculation of fluid flows with limited use of computer storage. *Argonne National Laboratory Technical Report* (1983) **ANL**:83-87.

[11] Lonsdale R.D., An algebraic multigrid scheme for solving the Navier-Stokes equations on unstructured meshes. *Proc. 7th International Conference on Numerical Methods in Turbulent abd Laminar Flows* (1991) Stanford,CA 1432-1442.

[12] Webster R., An algebraic multigrid solver for Navier-Stokes problems. *International Journal Numerical Methods Fluids* (1994) **18**:761-780.

[13] Rhie C.M. and Chow W.L., A numerical study of the turbulent flow past an isolated airfoil with trailing edge separation *AIAA* (1983) **21**:1525-1532.

[14] Balay S.; Brown J.; Buschelman K.; Gropp W.D.; Kaushik D.; Knepley M.G.; McInnes L.C.; Smith B.F. and Zhang H., PETSc Web page, (2012).

[15] Ferziger J.H. and Peric M., Computational Methods for Fluid Dynamics, Springer, Berlin, 1996.